A Conserved Metabolic Network Regulates Titan Cell Formation in *Cryptococcus neoformans*

Pallavi S Phatak[1,2], Ishvarya Suresh[1*], Dhrumi Shah[1,2*], Mary Shejo[1], Sudharsan Mathivathanan[1] and Sriram Varahan[1,2#]

Affiliations:
[1]CSIR-Centre for Cellular and Molecular Biology, Uppal Road, Hyderabad 500007, India.

[2]Academy of Scientific and Innovative Research (AcSIR), Ghaziabad- 201002, India.

 # - Corresponding Author:
Dr. Sriram Varahan
Senior Scientist
CSIR-Centre for Cellular and Molecular Biology (CCMB)
Email: sriram.ccmb@csir.res.in

*** - Authors Contributed Equally**

Abstract

Cryptococcus neoformans is an opportunistic fungal pathogen that primarily causes pulmonary infections, with the potential to cause life-threatening infections including meningoencephalitis in immunocompromised individuals. Key virulence factors including polysaccharide capsule and melanin, facilitate immune evasion and tissue invasion in the host. Recently, Titan cell formation, has been defined as another important virulence factor of *C. neoformans* and plays a pivotal role in disease progression. Titan cells are defined as enlarged cells with a diameter of ≥10 µm and are highly polyploid with a significantly thicker capsule compared to the yeast morphotype. Despite the established role of Titan cells in *C. neoformans* pathogenesis, the mechanistic details governing their formation remain largely unresolved. The cyclic AMP–protein kinase A (cAMP-PKA) pathway has been shown to be an important regulator of virulence-associated processes, including capsule formation, melanin biosynthesis and Titan cell formation. However, the upstream signals, critical for the activation of cAMP-PKA pathway in the context of Titan cell formation remain poorly understood. In this study, for the first time, we demonstrate that the central carbon metabolic pathway, glycolysis, is critical for cAMP-dependent Titan cell formation in *C. neoformans*. Pharmacological and genetic perturbation of glycolysis significantly attenuated Titan cell formation. Remarkably, exogenous addition of cAMP completely reversed the Titan cell defects observed during glycolysis perturbation. These findings establish a novel regulatory axis wherein central carbon metabolism orchestrates morphogenetic switching in *C. neoformans* by regulating the activity of the well conserved cAMP-PKA pathway, providing new insights into the metabolic control of *C. neoformans* dimorphism.

Importance

A leading opportunistic fungal pathogen, *Cryptococcus neoformans* poses a significant threat to human health, causing severe pulmonary and potentially fatal meningoencephalitis in immunocompromised patients. One of the key virulence factors of *C. neoformans* is Titan cell formation. However, the mechanisms driving Titan cell formation remains largely uncharacterized. While the cAMP-PKA pathway is recognized for its role in regulating virulence and Titanization, the upstream signaling cues needed for the activation of this pathway, in this context have been poorly understood. Our study uniquely demonstrates that glycolysis, a central carbon metabolic pathway, is critical for cAMP-dependent Titan cell formation. This establishes a novel regulatory axis where central carbon metabolism orchestrates this morphogenetic switch *via* the conserved cAMP-PKA pathway. Understanding these metabolic requirements offers crucial insights into the regulation of *C. neoformans* pathogenesis.

Key words: *Cryptococcus neoformans*, Capsule, Melanin, Titan cell formation, cAMP-PKA pathway, Glycolysis

Introduction

Cryptococcus neoformans is an opportunistic fungal pathogen that significantly impacts global public health, and causes life-threatening infections especially in immunocompromised individuals [1]. This pathogen is responsible for causing cryptococcosis that primarily manifests as a pulmonary infection but can disseminate to cause severe meningoencephalitis [2,3]. With an estimated 220,000 cases of cryptococcal meningitis occurring annually worldwide, resulting in approximately 180,000 deaths, *C. neoformans* has been designated as a critical priority fungal pathogen by the World Health Organization (WHO) [1,2]. The pathogenicity of *C. neoformans* is attributed to several well-characterized virulence factors that facilitate immune evasion and tissue invasion in the host [4]. The polysaccharide capsule, composed primarily of glucuronoxylomannan and galactoxylomannan, serves as a major virulence determinant by inhibiting phagocytosis and modulating the host immune response in favour of *C. neoformans* survival [5,6]. Additionally, melanin production through laccase-mediated oxidation of phenolic compounds, provides protection against oxidative stress and antimicrobial peptides, contributing to *C. neoformans* survival within the host [7,8]. In recent years, morphological plasticity has emerged as another critical virulence mechanism in *C. neoformans* [9]. While the organism typically exists as a budding yeast with cells ranging from 5-7 µm in diameter, several studies have shown that, upon host entry, *C. neoformans* undergoes a dramatic morphological transition resulting in the formation of unusually large cells known as 'Titan cells' [10–12]. Titan cells are defined as enlarged cells with a diameter of ≥10 µm (with some cells reaching sizes up to ~100 µm) [12]. Several studies have shown that Titan cells are resistant to phagocytosis as well as oxidative and nitrosative stresses within the host [11,13,14]. Similarly, *in vivo* studies suggest that Titan cells play a pivotal role in cryptococcal dissemination and disease progression [9,15]. Apart from increased cell size, Titan cells exhibit a high degree of polyploidy, a significantly thickened cell wall and capsule with an altered composition [12,13,16]. Titan cells also exhibit significant variations in homeostatic cellular processes compared to typical yeast cells, including alterations in cell cycle progression with an extended G2 phase and G2/M arrest [17,18]. The formation of Titan cells is associated with endoreduplication leading to polyploidy, which is proposed to be an important driver of Titanization [18,19].

Cyclic adenosine-3',5'-monophosphate-protein kinase A (cAMP-PKA) pathway is a highly conserved eukaryotic signalling cascade that regulates diverse cellular processes, including stress responses, metabolic adaptation, and morphogenetic transitions in various fungal species [20–22]. cAMP-PKA pathway is highly responsive to nutrient availability, specifically glucose levels and glycolytic flux and regulates various cellular processes in response to these metabolic cues [20,23]. In *C. neoformans*, cAMP-PKA pathway has emerged as a central regulator of key virulence factors including capsule formation, melanin biosynthesis and Titan cell formation [20,24,25]. Deletion strains that lack the genes encoding various cAMP-PKA pathway components, such as Cac1 (adenylate cyclase) or Pka1 (catalytic subunit of PKA), are unable to undergo Titanization both *in vitro* and *in vivo* [19,25–27]. Recently, a series of landmark studies have established that *in vitro* Titanization assays results in the reproducible generation of Titan cells that faithfully recapitulate the various biological signatures of Titan cells that are generated *in vivo* [26–28]. Interestingly, one of these studies showed that several glycolytic genes were upregulated under Titan cell inducing conditions suggesting a possible link between central carbon metabolism and Titan cell formation [27]. However, the precise

role of glycolysis in the context of Titan cell formation remains unexplored. Interestingly, the link between glycolysis and cAMP-PKA signalling has been well-established in the model fungi *Saccharomyces cerevisiae*, wherein the glycolytic intermediate, fructose-1,6-bisphosphate (FBP) directly activates the cAMP-PKA pathway through Ras2 activation [29]. Given that glycolysis and cAMP-PKA pathway are highly conserved across multiple fungal species, we hypothesized that a similar regulatory connection likely exists between these two processes in *C. neoformans*, specifically in the context of Titan cell formation.

Our findings reveal a critical role of central carbon metabolism, particularly glycolysis, in regulating Titan cell formation in *C. neoformans*. Our study demonstrates that perturbation of glycolysis using inhibitors or pertinent knockout strains, significantly reduced Titan cell formation. Furthermore, we observed that perturbation of glycolysis negatively affects the expression of cAMP-PKA pathway regulated genes involved in capsule formation and melanin biosynthesis [30,31]. Remarkably, exogenous supplementation of cAMP effectively rescued the Titan cell formation defects resulting from glycolysis perturbation, establishing a novel regulatory axis linking glycolysis and cAMP-PKA pathway in the context of Titan cell formation in *C. neoformans*. Additionally, our study, for the first time, demonstrates a direct role of melanin biosynthesis during Titan cell formation suggesting a possible interdependency between these two well-established virulence factors. Taken together, our findings advance our understanding of how conserved metabolic events orchestrate fungal morphogenesis by regulating a well-conserved signalling module in the critical priority fungal pathogen, *C. neoformans*.

Results

Perturbation of Glycolysis Attenuates Titan Cell Formation in *C. neoformans*:

Among a range of different morphotypes exhibited by *C. neoformans* [32,33], Titan cells, defined as cells with a diameter of ≥10 µm, represent an important virulence lifestyle critical for host pathogenesis [9,11]. Previous studies have shown that despite their increased size, Titan cells are metabolically active and exhibit significant variations in a variety of homeostatic cellular processes compared to the yeast cells of *C. neoformans* [34]. Titan cell formation is associated with altered cell cycle wherein cells are observed to have extended G2 phase and G2/M arrest [17]. Additionally, endoreduplication which results in polyploidy, is proposed to be an important driver of Titanization in *C. neoformans* [19]. Titan cells also possess a thicker cell wall and capsule with a significantly altered composition, compared to the yeast cells (cells with a diameter of 5-7 µm) [16,26]. Several studies have suggested a strong interdependency between cellular metabolism and changes in cell size, ploidy or cell envelope composition [35–38]. Importantly, glycolysis plays a central role in the generation of precursors needed for the biosynthesis of various cell wall sugars (glucans, mannan, glucosamine, xylose, galactose etc.), nucleic acids, and lipids [39]. Similarly, various studies have demonstrated a critical role for glycolysis in the regulation of cell cycle progression across different species [35,37]. Despite the fact that Titan cell formation in *C. neoformans* exhibits all the aforesaid changes including increase in cell size, alteration in cell cycle progression and variation in cell envelope architecture, the role of central carbon metabolic pathways including glycolysis has not been explored in this context. Interestingly, a previous study showed that the expression of multiple

180 glycolysis genes under Titan cell inducing conditions were significantly upregulated
181 suggesting a potential role for glycolysis in Titan cell formation [27].
182
183 To investigate the functional requirement of glycolysis in Titan cell formation, we tested the
184 ability of *C. neoformans* to undergo Titanization, using the previously established *in vitro* Titan
185 cell assay [27]. Briefly, wild-type *C. neoformans* strain H99 was cultured in Titan Cell Medium
186 (TCM) in the presence and absence of sub-inhibitory concentrations of two well-established
187 glycolysis inhibitors, 2-Deoxy-D-glucose (2DG) and sodium citrate (NaCi), which target the
188 early and rate-limiting steps of the glycolysis pathway and Titan cell formation was
189 subsequently assessed [27] (Fig. 1A). 2DG, a glucose analogue, acts as a competitive
190 inhibitor of hexokinase (Hxk) and phosphoglucose isomerase (Pgi), thereby perturbing
191 glycolysis at its initial steps [40]. Similarly, NaCi, interferes with the activity of
192 phosphofructokinase (Pfk), which is a key rate-limiting enzyme in the glycolysis pathway [41].
193 Previous studies have shown that when *C. neoformans* are grown in Titan cell inducing
194 medium, a heterogeneous population of cells emerge wherein the cell size ranges from 2 µm
195 to ≥10 µm, and the cells that 2-3 µm in diameter have been reported as Titanides [28,42]. In
196 our study, we focused on the typical yeast cell population, defined as those cells with cell sizes
197 ranging from 5 µm to 7 µm, and the cells that ≥10 µm are designated as Titan cells. The
198 percentage of Titan cells was quantified as the ratio of Titan cells (≥10 µm) to the total number
199 of cells (≥5 µm). Our data clearly demonstrates that sub-inhibitory concentrations of 2DG and
200 NaCi significantly attenuate the ability of *C. neoformans* to undergo Titan cell formation (Fig.
201 1B, C). To rule out the possibility that the phenotype we observed is due to a general growth
202 defect, we carried out growth curve analysis of *C. neoformans* in TCM, in the presence and
203 absence of glycolysis inhibitors. Our results clearly demonstrate that the reduction in Titan cell
204 formation is not due to a general growth defect, as presence of sub-inhibitory concentrations
205 of 2DG and NaCi did not affect the overall growth of the wild-type strain (Fig. 1D). Titan cells
206 are known to have a thicker and more complex capsule structure compared to the capsule of
207 yeast cells. Additionally, in the field, Titan cells have been defined by their cell size
208 either including or excluding the capsule [13]. Increased capsule expansion is thought to be
209 an important morphological hallmark of Titan cells, and given this, we wanted to assess
210 whether the perturbation of glycolysis affects Titan cell associated capsule thickness, and
211 consequently, overall cell size including the capsule. In order to do this, wild-type cells were
212 grown in TCM in the presence and absence of sub-inhibitory concentrations of glycolysis
213 inhibitors and capsule was visualized using India ink staining and total cell diameter including
214 the capsule was quantified. Our data shows that the addition of 2DG or NaCi resulted in a
215 significant reduction in overall capsule thickness and total cell diameter (Fig. 1E, F). This
216 demonstrates that the perturbation of glycolysis disrupts Titan cell associated capsule
217 expansion.
218
219 Given that, 2DG and NaCi exhibited a strong inhibitory effect on Titan cell formation, we
220 wanted to corroborate these observations by using pertinent genetic knockout strains that are
221 compromised in their ability to metabolize glucose *via* glycolysis [43]. In order to do this, we
222 tested the ability of knockout strains which lack the genes that encode for enzymes that are
223 involved in the glycolysis pathway including *hxk1* (Hexokinase 1)*, hxk2* (Hexokinase 2) and
224 *pyk1* (Pyruvate kinase 1) [43] (Fig. 2A). Specifically, *hxk1* and *hxk2* encode for enzymes that
225 catalyse the phosphorylation of glucose to glucose-6-phosphate, the initial step in glycolysis,
226 while *pyk1* encodes for the enzyme responsible for converting phosphoenolpyruvate to
227 pyruvate. Briefly, *hxk1*Δ*, hxk2*Δ *and pyk1*Δ (*hxk1*Δ refers to the *hxk1* knockout strain, *hxk2*Δ

228 refers to the *hxk2* knockout strain and *pyk1*Δ refers to the *pyk1* knockout strain) along with the
229 wild-type were cultured in TCM and incubated at 37°C under 5% CO_2 for 72 hours. Cells were
230 imaged using bright field microscopy, and percentage of Titan cells was quantified as the ratio
231 of Titan cells (≥10 µm) to the total number of cells (≥5 µm). Our result demonstrates that the
232 deletion of *hxk2* and *pyk1* resulted in a significant reduction in Titan cell formation, compared
233 to the wild-type strain (Fig. 2B). Interestingly, deletion of *hxk1* did result in the attenuation of
234 Titan cell formation compared to the wild-type strain, albeit to a lesser extent compared to the
235 deletion of *hxk2* and *pyk1* (Fig. 2B and C). To rule out the possibility that the phenotype we
236 observed is due to a general growth defect, we performed growth curve analysis of the wild-
237 type and knockout strains (*hxk1*Δ*, hxk2*Δ *and pyk1*Δ*)* in TCM. Our data suggests that the
238 reduction in Titan cell formation is not due to general growth defects as the mutants were able
239 to grow similar to the wild-type strain in TCM (Fig. 2D).
240
241 Given that the perturbation of glycolysis using 2DG or NaCi leads to reduced Titan cell
242 associated capsule size and overall cell diameter in the wild-type, we wanted to corroborate
243 these observations by using pertinent genetic knockout strains (*hxk1*Δ*, hxk2*Δ *and pyk1*Δ*)* that
244 are compromised in their ability to undergo glycolysis. In order to do this, glycolysis knockout
245 strains including *hxk1*Δ*, hxk2*Δ *and pyk1*Δ along with the wild-type were cultured in TCM and
246 capsule was visualized using India ink staining and total cell diameter was measured. Bright
247 field microscopy revealed that glycolysis knockout strains exhibited a significant decrease in
248 total cell diameter (which includes both the cell body and the capsule) compared to the wild-
249 type strain (Fig. 2E, F). Taken together, our results clearly demonstrate that the ability of *C.*
250 *neoformans* to efficiently metabolize glucose *via* glycolysis is critical for Titan cell formation.
251
252 **Perturbation of Glycolysis Affects cAMP-PKA Signalling in Titan Cell Inducing**
253 **Conditions:**
254
255 Our data clearly demonstrates that the perturbation of glycolysis using inhibitors or pertinent
256 knockout strains attenuates Titan cell formation in *C. neoformans*. Several studies have
257 established that fungi use different pathways to sense nutrient availability and modulate their
258 metabolic state in order to regulate growth and proliferation [44,45]. For example, glucose
259 availability and the glycolytic flux is sensed by the conserved signalling pathway, cyclic-AMP-
260 Protein Kinase A (cAMP-PKA) pathway in *S. cerevisiae* and it has been shown that active
261 glycolysis is critical for the full activation of this pathway [23,29]. Specifically, the glycolysis
262 intermediate fructose-1,6-bisphosphate is known to directly activate the cAMP-PKA pathway
263 *via* Ras2 activation [29]. In *C. neoformans,* cAMP-PKA pathway is known to play an important
264 role in host pathogenesis by regulating three critical virulence factors including capsule
265 formation, melanin biosynthesis and Titan cell formation [20,46,47]. cAMP-PKA pathway is a
266 central regulator of Titan cell formation in *C. neoformans* and multiple studies have shown that
267 the strains carrying deletions of genes that encode for cAMP-PKA pathway components
268 including, *cac1* which encodes for adenylate cyclase or *pka1* which encodes for the catalytic
269 subunit of PKA are unable to undergo Titanization *in vitro* and *in vivo* conditions [20,26,27].
270 Given the fundamental and highly conserved nature of the cAMP-PKA pathway across various
271 fungal species [20,48,49], we hypothesized that the glycolysis-dependent regulation of Titan
272 cell formation is mediated through the cAMP-PKA pathway. To test this hypothesis, we
273 analysed the gene expression of known downstream effectors of cAMP-PKA pathway in *C.*

274 *neoformans* [30,31], in glycolysis knockout strains, compared to the wild-type, under Titan cell
275 inducing conditions.
276
277 In order to do this, we measured the expression of cAMP-PKA pathway regulated genes
278 involved in capsule biosynthesis including *cap10* and *nrg1* (Fig. 3A, C). *cap10* is involved in
279 the biosynthesis of polysaccharide capsule in *C. neoformans* whereas *nrg1* encodes for a
280 transcription factor that regulates the expression of genes involved in capsule biosynthesis
281 [30,31] (Fig. 3A). To determine the relative expression of *cap10* and *nrg1,* glycolysis knockout
282 strains including *hxk1*Δ, *hxk2*Δ and *pyk1*Δ along with the wild-type strain were cultured in TCM
283 and incubated at 37°C under 5% CO_2 for 72 hours, following which total RNA was extracted
284 and gene expression levels were quantified using RT-qPCR. Our data shows that the
285 expression of *cap10* and *nrg1* were significantly downregulated in *hxk2*Δ and *pyk1*Δ as
286 compared to wild-type strain (Fig 3B). Interestingly, expression of these genes remained
287 unaffected in *hxk1*Δ strain (Fig. 3B). Similarly, we monitored the expression of *lac1 and lac2*
288 in glycolysis knockout strains including *hxk1*Δ, *hxk2*Δ *and pyk1*Δ along with the wild-type strain
289 in Titan cell inducing conditions. In *C. neoformans*, both *lac1 and lac2* encodes for the laccase
290 enzyme which catalyses an important step in melanin biosynthesis (Fig. 3C) [31]. Briefly,
291 glycolysis knockout strains including *hxk1*Δ, *hxk2*Δ *and pyk1*Δ*,* along with the wild-type strain
292 were cultured in TCM and incubated at 37°C under 5% CO_2 for 72 hours, following which total
293 RNA was extracted and gene expression levels were quantified using RT-qPCR. Our results
294 indicate that both *lac1 and lac2* were significantly downregulated *hxk2*Δ and *pyk1*Δ compared
295 to wild-type strain (Fig. 3D). Interestingly, expression of these genes remained unaffected in
296 *hxk1*Δ strain (Fig. 3D). Overall, these results indicate that the perturbation of glycolysis directly
297 influences the expression of genes which are regulated by cAMP-PKA pathway. This suggests
298 that active glycolytic flux might be important for the robust activation of the cAMP-PKA
299 pathway and its downstream regulon, under Titan cell inducing conditions.
300

301 **Glycolysis Orchestrates Titan Cell Formation in a cAMP-PKA Dependent**
302 **Manner:**
303

304 Our RT-qPCR results clearly demonstrated that the perturbation of glycolysis negatively
305 affects several downstream targets of cAMP-PKA pathway under Titan cell inducing
306 conditions. It is known in *S. cerevisiae* that active glycolytic flux is one of the critical upstream
307 events needed for the biosynthesis of cAMP which in turn is critical for the complete activation
308 of the cAMP-PKA pathway [23,29] (Fig. 4A). Given the conserved nature of this signalling
309 pathway, we hypothesized that active glycolytic flux might be critical for the production of
310 cAMP under Titan cell inducing conditions in *C. neoformans* as well and its perturbation results
311 in the downregulation of genes that are activated by the cAMP-PKA pathway. To test this
312 hypothesis, we performed cAMP-add back assays wherein glycolysis knockout strains
313 including *hxk2*Δ *and pyk1*Δ along with wild-type strain were cultured in TCM with and without
314 the exogenous supplementation of cAMP (10mM) and incubated for 72 hours at 37°C under
315 5% CO_2. Cells were imaged using bright field microscopy, and percentage of Titan cells was
316 quantified as the ratio of Titan cells (≥10 μm) to the total number of cells (≥5 μm). Remarkably,
317 exogenous supplementation of cAMP significantly rescued the Titan cell formation defect
318 observed in *hxk2*Δ *and pyk1*Δ strains (Fig. 4B, C). The percentage of Titan cells were
319 significantly higher in the cAMP treated *hxk2*Δ *and pyk1*Δ strains compared to the untreated
320 controls, reaching levels comparable to the wild-type strain (Fig. 4B, C).

321 cAMP-PKA pathway is a known positive regulator of capsule formation in *C. neoformans* [50].
322 Given that exogenous supplementation of cAMP significantly rescues the Titan cell formation
323 defects observed in the glycolysis knockout strains, we wanted to assess whether cAMP add-
324 back rescues Titan cell associated capsule thickness, and consequently, overall cell size
325 including the capsule. In order to do this, glycolysis knockout strains including *hxk2*Δ *and*
326 *pyk1*Δ along with the wild-type strain were cultured in TCM with and without exogenous
327 supplementation of cAMP (10mM) and incubated for 72 hours at 37°C under 5% CO_2. Capsule
328 was visualized using India ink staining and total cell diameter was measured. Our data
329 demonstrates that the exogenous supplementation of cAMP leads to significant increase in
330 capsule thickness and subsequent increase in the total cell diameter of *hxk2*Δ *and pyk1*Δ
331 strains compared to the untreated cultures of *hxk2*Δ *and pyk1*Δ strains, reaching levels
332 comparable to the wild-type strain (Fig. 4D, E). Collectively, our results indicate that glycolysis
333 regulates Titan cell formation through the activation of the cAMP-PKA pathway.
334
335 **Melanin Biosynthesis is Critical for Titan Cell Formation in *C. neoformans*:**
336
337 Our previous results indicate that glycolysis is critical for Titan cell formation through the
338 activation of the cAMP-PKA pathway in *C. neoformans*. Specifically, our RT-qPCR results
339 demonstrated that under Titan cell inducing conditions, functional glycolysis is essential for
340 the expression of genes involved in melanin biosynthesis including *lac1* and *lac2*, in a cAMP-
341 PKA pathway dependent manner (Fig. 5A). Although in *C. neoformans,* melanin is a known
342 virulence factor that contributes towards the host pathogenesis of this fungal pathogen, its
343 direct involvement in Titan cell formation remains unexplored. In order to determine whether
344 the reduced expression of genes involved in melanin biosynthesis directly contributes towards
345 the attenuation of Titan cell formation under glycolysis perturbation, we tested the ability of a
346 knockout strain (*lac1*Δ) which is impaired in melanin biosynthesis [46], to undergo Titan cell
347 formation. Briefly, *lac1*Δ strain along with the wild-type strain were cultured in TCM and
348 incubated at 37°C under 5% CO_2, for 72 hours. Cells were imaged using bright field
349 microscopy, and percentage of Titan cells was quantified as the ratio of Titan cells (≥10 µm)
350 to the total number of cells (≥5 µm). Our results demonstrate that the deletion of *lac1* resulted
351 in a significant reduction in Titan cell formation, compared to the wild-type strain (Fig. 5B). In
352 order to rule out whether the reduction in Titan cell formation in *lac1*Δ strain is due to a general
353 growth defect, we performed a growth curve analysis wherein overnight grown culture of
354 knockout strains (*lac1*Δ*)* along with wild-type strain were diluted to OD_{600}=0.01 in TCM and
355 allowed to grow at 37°C for 24 hours. OD_{600} was recorded at 3 hours intervals (Fig. 5C). Our
356 data suggests that the reduction in Titan cell formation is not due to general growth defects as
357 the mutant was able to grow similar to the wild-type strains in TCM
358
359 Additionally, we measured Titan cell associated capsule expansion and total cell diameter
360 (including the capsule thickness) for *lac1*Δ strain in Titan cell inducing conditions, similar to
361 our previous experiments. *lac1*Δ along with the wild-type strain were cultured in TCM and
362 incubated at 37°C under 5% CO_2 for 72 hours. Capsule was visualized using India ink staining
363 and total cell diameter was measured. Bright field microscopy revealed that *lac1*Δ exhibited a
364 significant decrease in total cell diameter which includes both the cell body and the
365 surrounding capsule relative to the wild-type strain (Fig. 5D). These findings, for the first time,
366 establish a direct role for melanin biosynthesis during Titan cell formation in *C. neoformans*,
367 highlighting the regulatory interdependencies of these virulence factors.

Discussion

Our findings provide compelling evidence for a conserved regulatory axis that links central carbon metabolism, specifically glycolysis and cAMP-PKA pathway in the regulation of Titan cell formation in *C. neoformans.* Even though several studies have demonstrated that cAMP-PKA pathway is critical for Titan cell formation [12,19,20,51], the upstream signals that are required for the activation of this pathway during Titan cell formation remains poorly understood. Titan cells exhibit dramatically altered cellular and morphological changes compared to the yeast morphotype and these include increase in cell size, polyploidy resulting from endoreduplication, thicker cellular envelope (cell wall and polysaccharide capsule) with altered composition [12,13]. Importantly, glycolysis plays an critical role in generating various precursors required for cell wall and capsule biosynthesis, and the role of glycolysis in regulating cell size and cell cycle progression in various organisms including multiple fungal species is well established [36,37,39]. A recent study that reported the successful generation of *in vitro* Titan cells which are remarkably similar to the Titan cells that are formed *in vivo*, during *C. neoformans* infections, demonstrated that *in vitro* Titan cells have increased expression of several glycolytic genes [27]. Given these observations, we hypothesized that glycolysis might play an important role in the regulation of Titan cell formation in *C. neoformans*. The inhibition of glycolysis with sub-inhibitory concentrations of 2DG and NaCi significantly reduced Titan cell formation, providing strong evidence for the metabolic dependency of this morphogenetic process. These findings were further supported by the results from Titan cell assays using pertinent glycolysis knockout strains wherein *hxk1*Δ (*hxk1*Δ refers to the *hxk1* knockout strain) strain showed a marginal reduction in Titan cell formation compared to the wild-type whereas *hxk2*Δ (*hxk2*Δ refers to the *hxk2* knockout strain) and *pyk1*Δ (*pyk1*Δ refers to the *pyk1* knockout strain) strains showed a substantial reduction in Titan cell formation compared to the wild-type. The differential effects observed among the various deletion strains, with *hxk2*Δ and *pyk1*Δ showing a stronger Titan cell formation defect compared to *hxk1*Δ, likely reflects the distinct role of these enzymes in glucose metabolism and their relative contributions to the overall glycolytic flux [43]. Previous studies have shown that *hxk2* encodes the predominant hexokinase isoform in *S. cerevisiae* (Karri et al., 2024). Variations observed in Titan cell formation between *hxk1*Δ and *hxk2*Δ strains may similarly reflect a dominant role for *hxk2* during *C. neoformans* glycolysis. Pyk1 is the only known pyruvate kinase in *C. neoformans*, making it indispensable for functional glycolysis [43]. Consequently, the deletion of *pyk1* resulted in a significant reduction in Titan cell formation.

Our study demonstrates that glycolysis regulates Titan cell formation through the cAMP-PKA signalling pathway (Fig. 6). Interestingly, in *S. cerevisiae*, the cAMP-PKA pathway is remarkably responsive to both glucose levels and glycolytic flux. This regulation is primarily mediated by glucose, which activates the pathway *via* the G-protein coupled receptor Gpr1 [20,52]. Additionally, a key glycolytic intermediate, fructose-1,6-bisphosphate is recognized as an activator of the cAMP-PKA cascade, exerting its effect through interaction with Ras2 [29]. Given the conserved nature of glycolysis and cAMP-PKA pathway across different fungal species, we hypothesised that the effect of glycolysis perturbation on Titan cell formation is mediated through activation of cAMP-PKA pathway. Our results elucidate a transcriptional downregulation of cAMP-PKA target genes (*cap10, nrg1, lac1, and lac2*) in pertinent glycolysis knockout strains including *hxk2*Δ and *pyk1*Δ compared to the wild-type strain. This provides

414 further evidence supporting a regulatory link between glycolysis and the cAMP-PKA pathway
415 in *C. neoformans*, specifically in the context of Titan cell formation. Remarkably, exogenous
416 supplementation of cAMP rescues Titan cell formation defects exhibited by glycolysis
417 knockout strains (*hxk2*Δ and *pyk1*Δ*)*, strongly suggesting that glycolysis functions upstream
418 of cAMP-PKA activation, establishing a metabolic checkpoint for this morphogenetic transition.
419 It is likely that a glycolysis intermediate activates the cAMP-PKA pathway in *C. neoformans*,
420 a mechanism similar to that observed in *S. cerevisiae*. Further studies are required to delineate
421 the precise molecular mechanisms underlying glycolysis mediated regulation of cAMP-PKA
422 pathway activation under Titan cell inducing conditions.
423
424 *C. neoformans* is a Crabtree-negative organism, implying a tight coupling between glycolysis
425 and respiration [53]. Interestingly, a study by Black *et al*., showed a positive correlation
426 between mitochondrial respiration and expression of virulence factors of *C. neoformans*
427 including capsule and melanin [54]. Respiration, particularly the Electron Transport Chain
428 (ETC) within the mitochondria, is the primary source of endogenous Reactive Oxygen Species
429 (ROS), which is a known activator of Titan cell formation [34,55]. In our study, the presence of
430 sodium azide in the Titan Cell Medium (TCM) is particularly relevant in this context [27].
431 Sodium azide inhibits catalase, an enzyme vital for maintaining redox homeostasis by
432 detoxifying harmful ROS [27,56]. Consequently, catalase inhibition would lead to an increase
433 in intracellular ROS levels within *C. neoformans*. Considering these factors, the observed
434 effect of functional glycolysis on Titan cell formation could likely be due to the fact that active
435 glycolysis would increase TCA-dependent respiration, and this combined with sodium azide-
436 mediated catalase inhibition, would result in an amplified accumulation of ROS. Importantly,
437 elevated ROS levels are known to cause DNA damage, which can trigger cell cycle arrest
438 after the G2 phase [57]. This G2 arrest is a prerequisite for endoreduplication, a hallmark of
439 Titan cell formation, characterized by DNA replication without subsequent cell division, leading
440 to polyploidy and increased cell size [17,58]. This suggests a potential mechanism wherein
441 glycolysis perturbation could potentially lead to a subsequent decrease in ROS levels which
442 in turn results in reduced Titan cell formation. Furthermore, multiple studies indicate that the
443 cAMP-PKA pathway affects ROS homeostasis, partly by affecting mitochondrial biogenesis
444 and function [50,59]. Given that the cAMP-PKA pathway is also a central regulator of Titan
445 cell formation, it is plausible that it acts as an integrator, sensing metabolic state (including
446 glucose flux), influencing mitochondrial activity, modulating ROS levels, and thereby
447 coordinating the endoreduplication process essential for Titanization. This posits a complex
448 interplay between upstream metabolic cues and cAMP-PKA pathway which in turn drives Titan
449 cell formation in *C. neoformans*.
450
451 In *C. neoformans*, melanin is a well-established and critical virulence factor, that primarily
452 serves as an antioxidant, actively scavenging excessive ROS to maintain redox homeostasis
453 [60]. Our results indicated that glycolysis is critical for Titanization through the cAMP-PKA
454 pathway, and functional glycolysis is essential for the cAMP-PKA-dependent expression of
455 melanin biosynthesis genes including *lac1* and *lac2*. However, to the best of our knowledge,
456 no studies have reported the direct involvement of melanin biosynthesis during Titan cell
457 formation. To bridge this knowledge gap and ascertain whether reduced melanin production
458 directly contributes to the observed attenuation of Titan cell formation under glycolysis
459 perturbation, we specifically tested the ability of a knockout strain (*lac1*Δ) which is impaired in
460 melanin biosynthesis [46], to undergo Titan cell formation. Interestingly, our results
461 demonstrate that the deletion of *lac1* leads to a significant reduction in Titan cell formation.

These findings, for the first time, establish a direct and indispensable role for melanin biosynthesis in Titan cell formation in *C. neoformans*. Given that ROS-induced DNA damage is critical for endoreduplication [34,56] and subsequent Titan cell formation under *in vitro* conditions, melanin might be playing an important role in preventing excessive ROS accumulation, ensuring that ROS levels remain within a specific threshold needed for Titan cell induction. This critical balance is important, as insufficient ROS may not trigger the necessary responses needed for Titan cell formation, while excessive ROS can lead to pleotropic cellular changes that can potentially inhibit Titan cell formation. A recent study shows that deletion of *gsh2*, a gene encoding for glutathione synthetase, a key enzyme involved in redox homeostasis of *C. neoformans*, attenuates Titan cell formation further strengthening the aforesaid hypothesis. Furthermore, the redox state of the cell, directly influenced by ROS levels, is critical for melanin biosynthesis itself, creating a feedback loop where melanin production is modulated to maintain redox homeostasis [61]. While melanin has been extensively studied as a protective pigment that enhances resistance to oxidative stress and antimicrobial compounds [62], our results unveil a novel role in facilitating Titan cell formation. Future investigations will be essential to precisely delineate the molecular mechanisms by which melanin directly contributes to the regulation of Titan cell formation.

In conclusion, our study establishes glycolysis as a critical metabolic pathway that modulates Titan cell formation in *C. neoformans* through the regulation of the cAMP-PKA signalling. We demonstrate that this metabolic control extends to coordinate regulation of virulence factors, including the novel finding that melanin biosynthesis is directly required for Titanization. These findings provide new insights into the metabolic basis of morphogenetic transitions in *C. neoformans* and highlight the connections between central carbon metabolism and pathogenesis. Understanding these metabolic requirements not only advances our fundamental knowledge of *C. neoformans* biology but also reveals potential targets for therapeutic intervention against this opportunistic pathogen.

Materials and Methods

Strains and Media:

All strains used in this study are listed in Table 1. All experiments were performed using *Cryptococcus neoformans* var. grubii, serotype A, H99 wild-type, and its derivatives. The glycolysis knockout strains (*hxk1*Δ, *hxk2*Δ *and pyk1*Δ) and the strain defective in melanin biosynthesis (*lac1*Δ) were generously provided by Dr. Joeseph Heitman, Duke University, USA.

Yeast Peptone (YP) (1% (w/v) yeast extract, 2% (w/v) peptone) medium supplemented with glycerol was used for cryo-preservation of strains at -80°C. All the strains were recovered at 30°C on YPD Agar plates (1% (w/v) yeast extract, 2% (w/v) peptone, 2% (w/v) glucose, 2% (w/v) agar).

YPD broth containing 1% (w/v) yeast extract, 2% (w/v) peptone and 2% (w/v) glucose was used for the overnight growth of the cultures. Overnight cultures of various strains were grown in YPD broth and incubated at 37°C with continuous shaking at 200 Rotations Per Minute (RPM). Titan Cell Medium (TCM) containing 5% (w/v) SDA (Sabouraud), 5% (v/v) FBS (Fetal Bovine Serum), 15μM Sodium Azide and 50mM MOPS was used for all *in vitro* Titan cell assays.

509 **Table 1: *C. neoformans* Strains Used in this Study**

Strain	Genotype	References
Wild-type	*C. neofrormans* var. Grubii, serotype A, H99	[63]
*pyk1*Δ	*C. neofrormans* var. Grubii, serotype A, H99, *pyk1*Δ*::NEO,* (MPC31)	[43]
*hxk1*Δ	*C. neofrormans* var. Grubii, serotype A, H99, *hxk1*Δ*::NEO,* (MPC38)	[43]
*hxk2*Δ	*C. neofrormans* var. Grubii, serotype A, H99, *hxk2*Δ*::NAT,* (AI110)	[43]
*lac1*Δ	*C. neofrormans* var. Grubii, serotype A, H99, *lac1*Δ*::NAT,* (CHM3)	[46]

510

511 ***In Vitro* Titan Cell Assays:**

512 For *in vitro* Titan cell inducing assays, overnight grown cultures of different *C. neoformans*
513 strains (listed in Table 1) were inoculated in TCM at a cell density of 10^6 CFU per ml. For Titan
514 cell inducing assays with glycolysis inhibitors, cultures were grown in TCM at cell density of
515 10^6 CFU per ml with 0.025% (w/v) of 2-Deoxy-D-Glucose (2DG) and 0.5% (w/v) of Sodium
516 citrate for 72 hours at 37°C under 5% CO_2.
517

518 For cAMP add-back assays, wild-type and knockout strains of *C. neoformans* were cultured
519 in TCM at cell density of 10^6 CFU per ml in the presence and absence of 10mM cAMP for 72
520 hours at 37°C under 5% CO_2. Following 72 hours of incubation, cells were fixed and imaged
521 using Zeiss Apotome microscope. Cell diameter was measured using Zen 2.3 software and
522 Titan cell quantification was done. Titan cell percentage was calculated as a ratio of cells with
523 cell body diameter of ≥10 µm to total of cells (≥5µm). Statistical analysis was done using
524 GraphPad Prism (v 9.0). Statistical significance was performed with unpaired t-test and the
525 error bars represent the Standard Error of the Mean (SEM). All statistical comparison was
526 based on a minimum of three independent biological replicates.
527

528 **Capsule Visualization and Analysis:**

529 For visualization and analysis of capsule, overnight grown cultures of different *C. neoformans*
530 strains (listed in Table 1) were inoculated in TCM at cell density of 10^6 CFU per ml for 72 hours
531 at 37°C under 5% CO_2. Following 72 hours of incubation, cells were fixed and stained using
532 India Ink. Samples were imaged using Zeiss Apotome microscope. Capsule width was
533 measured using Zen 2.3 software. Statistical analysis was performed using GraphPad Prism
534 (v 9.0). Unpaired t-test was done to assess the statistical significance and error bars represent
535 SEM. All statistical comparison was based on a minimum of three independent biological
536 replicates.
537

538 **Quantitative Real Time Polymerase Chain Reaction (RT-qPCR) Assays:**

539 Wild-type and knockout strains (listed in Table 1) of *C. neoformans* were cultured in TCM at
540 cell density of 10^6 CFU per ml for 72 hours at 37°C under 5% CO_2. Total RNA was extracted
541 following 72 hours of incubation using the Ribopure RNA purification kit (yeast) (cat. #AM1926)
542 following the manufacturers instruction. cDNA biosynthesis was done using PrimeScript cDNA
543 biosynthesis kit (cat. #6110A). Primers used for RT-qPCR were designed using PrimeQuest
544 tool from Integrated DNA Technologies (IDT) and the Primers used in these experiments are

545 listed in Table 2. RT-qPCR was performed using iTaq Universal SYBR Green Master Mix (cat.
546 #1725121). Actin was used as housekeeping gene for normalization. The results were
547 analysed using the $2^{-\Delta\Delta CT}$ method and statistical analysis was done using unpaired t-test, with
548 error bars representing SEM. All statistical comparison was based on a minimum of three
549 independent biological replicates.
550

551 **Growth Curve Experiments:**

552 Overnight cultures of wild-type and knockout strains of *C. neoformans* (listed in Table 1) were
553 inoculated in TCM at OD_{600} of 0.01 and incubated at 37°C under continuous shaking conditions
554 at 200 RPM for 24 hours. OD_{600} was recorded at 3 hour intervals. For growth curve analysis
555 in presence of glycolysis inhibitors, overnight cultures were inoculated in TCM in the presence
556 and absence of 0.025% (w/v) of 2-Deoxy-D-Glucose (2DG) or 0.5% (w/v) of Sodium citrate
557 (NaCi) and incubated at 37°C under continuous shaking conditions at 200 RPM for 24 hours.
558 OD_{600} was recorded at 3 hour intervals. All the experiments were performed independently
559 thrice.
560

561 **Table 2: Primers Used in This Study**

Primer name	Description	5' to 3' Sequence
SV775	*Cryptococcus neoformans* Cap10 F1	TAACCTCACGGCTGACTCTA
SV776	*Cryptococcus neoformans* Cap10 R1	TTACCATCACCTCGCCAATC
SV777	*Cryptococcus neoformans* Nrg1 F1	CTAGTATCGCTCCTGAACATAGC
SV778	*Cryptococcus neoformans* Nrg1 R1	GAAGCCGAAAGTCCGTAAGA
SV781	*Cryptococcus neoformans* Lac1 F1	GCAACGAGTTCCAGGTGATAG
SV782	*Cryptococcus neoformans* Lac1 R1	GGTATCCTTTCTCACAGGGTTG
SV783	*Cryptococcus neoformans* Lac2 F1	AGTGTTGCTCTGGACTGTATG
SV784	*Cryptococcus neoformans* Lac2 R1	AGGCTCAGCGGTAGTAATAGA
SV795	*Cryptococcus neoformans* Actin F1	GCAGAACCGAGAGAAGATGAC
SV796	*Cryptococcus neoformans* Actin R1	CGGAAGCGTAAAGAGAGAGAAC

562
563
564
565
566
567
568
569

Acknowledgements

We extend our immense gratitude to Dr. Joseph Heitman and Mrs. Anna Floyd-Averette for generously providing the strains used in this study. We would like to thank Dr. Sunil Laxman (BRIC-inStem) for critical reading of our manuscript. We gratefully acknowledge the invaluable support and resources offered by CSIR-Centre for Cellular and Molecular Biology (CCMB) central facilities including Advanced Microscopy and Imaging facility (AMIF). PSP thanks Council of Scientific and Industrial Research (CSIR), India for her research fellowship. SV acknowledges funding from Indian Council of Medical Research (ICMR) (IIRPSG-2024-01-02717), India; Anusandhan National Research Foundation (ANRF) (SRG/2023/000470), India; Council of Scientific & Industrial Research (CSIR) (FTT070505), India; and DBT-Wellcome Trust India Alliance (IA/E/16/1/502996), India.

Author Contributions

Pallavi S Phatak: Investigation; Formal analysis; Visualization; Writing-original draft. **Ishvarya Suresh:** Investigation; Writing-original draft. **Dhrumi Shah:** Investigation; Writing-original draft. **Mary Shejo:** Investigation; Writing-original draft. **Sudharsan Mathivathanan:** Investigation. **Sriram Varahan:** Conceptualization; Supervision; Funding acquisition; Investigation; Formal analysis; Visualization; Writing-original draft; Writing-review and editing.

Conflict of Interest

The authors declare that they have no conflict of interests.

References

1. Zhao Y, Ye L, Zhao F, Zhang L, Lu Z, Chu T, et al. Cryptococcus neoformans, a global threat to human health. Infectious Diseases of Poverty. 2023. doi:10.1186/s40249-023-01073-4
2. Rajasingham R, Smith RM, Park BJ, Jarvis JN, Govender NP, Chiller TM, et al. Global burden of disease of HIV-associated cryptococcal meningitis: an updated analysis. Lancet Infect Dis. 2017;17: 873–881. doi:10.1016/S1473-3099(17)30243-8
3. Chen M, Xu Y, Hong N, Yang Y, Lei W, Du L, et al. Epidemiology of fungal infections in China. Frontiers of Medicine. 2018. doi:10.1007/s11684-017-0601-0
4. Zaragoza O. Basic principles of the virulence of Cryptococcus. Virulence. 2019. doi:10.1080/21505594.2019.1614383
5. Zaragoza O, Rodrigues ML, De Jesus M, Frases S, Dadachova E, Casadevall A. Chapter 4 The Capsule of the Fungal Pathogen Cryptococcus neoformans. Advances in Applied Microbiology. 2009. doi:10.1016/S0065-2164(09)01204-0
6. O'Meara TR, Andrew Alspaugh J. The Cryptococcus neoformans capsule: A sword and a shield. Clinical Microbiology Reviews. 2012. doi:10.1128/CMR.00001-12
7. Nosanchuk JD, Casadevall A. The contribution of melanin to microbial pathogenesis. Cellular Microbiology. 2003. doi:10.1046/j.1462-5814.2003.00268.x
8. Eisenman HC, Casadevall A. Synthesis and assembly of fungal melanin. Applied Microbiology and Biotechnology. 2012. doi:10.1007/s00253-011-3777-2
9. Okagaki LH, Strain AK, Nielsen JN, Charlier C, Baltes NJ, Chrétien F, et al. Cryptococcal cell morphology affects host cell interactions and pathogenicity. PLoS Pathog. 2010. doi:10.1371/journal.ppat.1000953
10. Cruickshank JG, Cavill R, Jelbert M. Cryptococcus neoformans of unusual morphology. Appl Microbiol. 1973. doi:10.1128/aem.25.2.309-312.1973
11. Crabtree JN, Okagaki LH, Wiesner DL, Strain AK, Nielsen JN, Nielsen K. Titan cell production enhances the virulence of Cryptococcus neoformans. Infect Immun. 2012. doi:10.1128/IAI.00507-12
12. Zhou X, Ballou ER. The Cryptococcus neoformans Titan Cell: From In Vivo Phenomenon to In Vitro Model. Current Clinical Microbiology Reports. 2018. doi:10.1007/s40588-018-0107-9
13. García-Rodas R, de Oliveira H, Trevijano-Contador N, Zaragoza O. Cryptococcal titan cells: When yeast cells are all grown up. Current Topics in Microbiology and Immunology. 2019. doi:10.1007/82_2018_145
14. Okagaki LH, Nielsen K. Titan cells confer protection from phagocytosis in Cryptococcus neoformans infections. Eukaryot Cell. 2012. doi:10.1128/EC.00121-12
15. García-Barbazán I, Trevijano-Contador N, Rueda C, de Andrés B, Pérez-Tavárez R, Herrero-Fernández I, et al. The formation of titan cells in Cryptococcus neoformans depends on the mouse strain and correlates with induction of Th2-type responses. Cell Microbiol. 2016. doi:10.1111/cmi.12488
16. Mukaremera L, Lee KK, Wagener J, Wiesner DL, Gow NAR, Nielsen K. Titan cell production in Cryptococcus neoformans reshapes the cell wall and capsule composition during infection. Cell Surf. 2018. doi:10.1016/j.tcsw.2017.12.001
17. Altamirano S, Li Z, Fu MS, Ding M, Fulton SR, Yoder JM, et al. The Cyclin Cln1 Controls Polyploid Titan Cell Formation following a Stress-Induced G2 Arrest in Cryptococcus. MBio. 2021. doi:10.1128/mBio.02509-21
18. Zaragoza O, Nielsen K. Titan cells in Cryptococcus neoformans: Cells with a giant impact. Current Opinion in Microbiology. 2013. doi:10.1016/j.mib.2013.03.006
19. Zaragoza O, Rocío GR, Nosanchuk JD, Cuenca-Estrella M, Rodríguez-Tudela JL, Casadevall A. Fungal cell gigantism during mammalian infection. PLoS Pathog. 2010. doi:10.1371/journal.ppat.1000945
20. Caza M, Kronstad JW. The cAMP/protein kinase a pathway regulates virulence and adaptation to host conditions in cryptococcus neoformans. Frontiers in Cellular and Infection Microbiology. 2019. doi:10.3389/fcimb.2019.00212
21. Pukkila-Worley R, Alspaugh JA. Cyclic AMP signaling in Cryptococcus neoformans. FEMS Yeast Research. 2004. doi:10.1016/S1567-1356(03)00241-1
22. D'Souza CA, Heitman J. Conserved cAMP signaling cascades regulate fungal development and virulence. FEMS Microbiology Reviews. 2001. doi:10.1016/S0168-6445(01)00058-4
23. Busti S, Coccetti P, Alberghina L, Vanoni M. Glucose signaling-mediated coordination of cell growth and cell cycle in Saccharomyces Cerevisiae. Sensors. 2010. doi:10.3390/s100606195
24. Alspaugh JA, Perfect JR, Heitman J. Cryptococcus neoformans mating and virulence are regulated by the G- protein α subunit GPA1 and cAMP. Genes Dev. 1997. doi:10.1101/gad.11.23.3206
25. D'Souza CA, Alspaugh JA, Yue C, Harashima T, Cox GM, Perfect JR, et al. Cyclic AMP-Dependent Protein Kinase Controls Virulence of the Fungal Pathogen Cryptococcus neoformans . Mol Cell Biol. 2001. doi:10.1128/mcb.21.9.3179-3191.2001
26. Hommel B, Mukaremera L, Cordero RJB, Coelho C, Desjardins CA, Sturny-Leclère A, et al. Titan cells formation in Cryptococcus neoformans is finely tuned by environmental conditions and modulated by positive and negative genetic regulators. PLoS Pathog. 2018. doi:10.1371/journal.ppat.1006982
27. Trevijano-Contador N, de Oliveira HC, García-Rodas R, Rossi SA, Llorente I, Zaballos Á, et al. Cryptococcus neoformans can form titan-like cells in vitro in response to multiple signals. PLoS Pathog. 2018. doi:10.1371/journal.ppat.1007007

28. Dambuza IM, Drake T, Chapuis A, Zhou X, Correia J, Taylor-Smith L, et al. The Cryptococcus neoformans Titan cell is an inducible and regulated morphotype underlying pathogenesis. PLoS Pathog. 2018. doi:10.1371/journal.ppat.1006978
29. Peeters K, Van Leemputte F, Fischer B, Bonini BM, Quezada H, Tsytlonok M, et al. Fructose-1,6-bisphosphate couples glycolytic flux to activation of Ras. Nat Commun. 2017. doi:10.1038/s41467-017-01019-z
30. Cramer KL, Gerrald QD, Nichols CB, Price MS, Alspaugh JA. Transcription factor Nrg1 mediates capsule formation, stress response, and pathogenesis in Cryptococcus neoformans. Eukaryot Cell. 2006. doi:10.1128/EC.00145-06
31. Pukkila-Worley R, Gerrald QD, Kraus PR, Boily MJ, Davis MJ, Giles SS, et al. Transcriptional network of multiple capsule and melanin genes governed by the Cryptococcus neoformans cyclic AMP cascade. Eukaryot Cell. 2005. doi:10.1128/EC.4.1.190-201.2005
32. Brown JC, Ballou ER. Is Cryptococcus neoformans a pleomorphic fungus? Curr Opin Microbiol. 2024;82: 102539. doi:10.1016/J.MIB.2024.102539
33. Stempinski PR, Gerbig GR, Greengo SD, Casadevall A. Last but not yeast-The many forms of Cryptococcus neoformans. PLoS Pathog. 2023. doi:10.1371/journal.ppat.1011048
34. García-Barbazán I, Torres-Cano A, García-Rodas R, Sachse M, Luque D, Megías D, et al. Accumulation of endogenous free radicals is required to induce titan-like cell formation in Cryptococcus neoformans. MBio. 2024. doi:10.1128/mbio.02549-23
35. Kalucka J, Missiaen R, Georgiadou M, Schoors S, Lange C, De Bock K, et al. Metabolic control of the cell cycle. Cell Cycle. 2015. doi:10.1080/15384101.2015.1090068
36. Cadart C, Heald R. Scaling of biosynthesis and metabolism with cell size. Mol Biol Cell. 2022. doi:10.1091/mbc.E21-12-0627
37. Diehl FF, Sapp KM, Vander Heiden MG. The bidirectional relationship between metabolism and cell cycle control. Trends in Cell Biology. 2024. doi:10.1016/j.tcb.2023.05.012
38. Sachla AJ, Helmann JD. Resource sharing between central metabolism and cell envelope synthesis. Current Opinion in Microbiology. 2021. doi:10.1016/j.mib.2021.01.015
39. Kierans SJ, Taylor CT. Glycolysis: A multifaceted metabolic pathway and signaling hub. J Biol Chem. 2024;300. doi:10.1016/j.jbc.2024.107906
40. Cramer FB, Woodward GE. 2-Desoxy-D-glucose as an antagonist of glucose in yeast fermentation. J Franklin Inst. 1952. doi:10.1016/0016-0032(52)90852-1
41. Yoshino M, Murakami K. AMP deaminase as a control system of glycolysis in yeast. Mechanism of the inhibition of glycolysis by fatty acid and citrate. J Biol Chem. 1982. doi:10.1016/s0021-9258(18)33871-7
42. Feldmesser M, Kress Y, Casadevall A. Dynamic changes in the morphology of Cryptococcus neoformans during murine pulmonary infection. Microbiology. 2001. doi:10.1099/00221287-147-8-2355
43. Price MS, Betancourt-Quiroz M, Price JL, Toffaletti DL, Vora H, Hu G, et al. Cryptococcus neoformans requires a functional glycolytic pathway for disease but not persistence in the host. MBio. 2011;2. doi:10.1128/MBIO.00103-11/SUPPL_FILE/MBIO.00103-11-S1.PDF
44. Yuan HX, Xiong Y, Guan KL. Nutrient Sensing, Metabolism, and Cell Growth Control. Molecular Cell. 2013. doi:10.1016/j.molcel.2013.01.019
45. Bahn YS, Xue C, Idnurm A, Rutherford JC, Heitman J, Cardenas ME. Sensing the environment: Lessons from fungi. Nature Reviews Microbiology. 2007. doi:10.1038/nrmicro1578
46. Hicks JK, D'Souza CA, Cox GM, Heitman J. Cyclic AMP-Dependent Protein Kinase Catalytic Subunits Have Divergent Roles in Virulence Factor Production in Two Varieties of the Fungal Pathogen Cryptococcus neoformans. Eukaryot Cell. 2004. doi:10.1128/EC.3.1.14-26.2004
47. Mahmood F;, Chen J-M;, Al-Huthaifi AM;, Al-Alawi AA;, Mahmood F, Chen J-M, et al. Roles of Different Signaling Pathways in Cryptococcus neoformans Virulence. J Fungi 2024, Vol 10, Page 786. 2024;10: 786. doi:10.3390/JOF10110786
48. Fuller KK, Rhodes JC. Protein kinase A and fungal virulence. Virulence. 2012. doi:10.4161/viru.19396
49. Yu PL, Rollins JA. The cAMP-dependent protein kinase A pathway perturbs autophagy and plays important roles in development and virulence of Sclerotinia sclerotiorum. Fungal Biol. 2022. doi:10.1016/j.funbio.2021.09.004
50. Leadsham JE, Gourlay CW. CAMP/PKA signaling balances respiratory activity with mitochondria dependent apoptosis via transcriptional regulation. BMC Cell Biol. 2010. doi:10.1186/1471-2121-11-92
51. Okagaki LH, Wang Y, Ballou ER, O'Meara TR, Bahn YS, Alspaugh JA, et al. Cryptococcal Titan Cell Formation Is Regulated by G-Protein Signaling in Response to Multiple Stimuli ∇. Eukaryot Cell. 2011. doi:10.1128/EC.05179-11
52. Xue Y, Batlle M, Hirsch JP. GPR1 encodes a putative G protein-coupled receptor that associates with the Gpa2p G(α) subunit and functions in a Ras-independent pathway. EMBO J. 1998;17: 1996–2007. doi:10.1093/EMBOJ/17.7.1996
53. Lev S, Li C, Desmarini D, Liuwantara D, Sorrell TC, Hawthorne WJ, et al. Monitoring glycolysis and respiration highlights metabolic inflexibility of cryptococcus neoformans. Pathogens. 2020. doi:10.3390/pathogens9090684
54. Black B, Lee C, Horianopoulos LC, Jung WH, Kronstad JW. Respiring to infect: Emerging links between mitochondria, the electron transport chain, and fungal pathogenesis. PLoS Pathog. 2021. doi:10.1371/journal.ppat.1009661
55. Zhao RZ, Jiang S, Zhang L, Yu Z Bin. Mitochondrial electron transport chain, ROS generation and

uncoupling (Review). International Journal of Molecular Medicine. 2019. doi:10.3892/ijmm.2019.4188

56. Ogino K, Kodama N, Nakajima M, Yamada A, Nakamura H, Nagase H, et al. Catalase catalyzes nitrotyrosine formation from sodium azide and hydrogen peroxide. Free Radic Res. 2001. doi:10.1080/10715760100301241

57. Chuang TC, Shao WS, Hsu SC, Lee SL, Kao MC, Wang V. Baicalein Induces G2/M Cell Cycle Arrest Associated with ROS Generation and CHK2 Activation in Highly Invasive Human Ovarian Cancer Cells. Molecules. 2023. doi:10.3390/molecules28031039

58. Maity S, Guchhait R, Pramanick K. Melatonin induces endoreduplication through oxidative DNA damage triggering lateral root formation in onions. Acta Physiol Plant. 2025;47: 1–13. doi:10.1007/S11738-024-03764-3/FIGURES/5

59. Bouchez C, Devin A. Mitochondrial biogenesis and mitochondrial reactive oxygen species (Ros): A complex relationship regulated by the camp/pka signaling pathway. Cells. 2019. doi:10.3390/cells8040287

60. Zadrag-Tecza R, Maślanka R, Bednarska S, Kwolek-Mirek M. Response Mechanisms to Oxidative Stress in Yeast and Filamentous Fungi. Stress Response Mech Fungi Theor Pract Asp. 2018; 1–34. doi:10.1007/978-3-030-00683-9_1

61. Black B, da Silva LBR, Hu G, Qu X, Smith DFQ, Magaña AA, et al. Glutathione-mediated redox regulation in Cryptococcus neoformans impacts virulence. Nat Microbiol 2024 98. 2024;9: 2084–2098. doi:10.1038/s41564-024-01721-x

62. Casadevall A, Rosas AL, Nosanchuk JD. Melanin and virulence in Cryptococcus neoformans. Current Opinion in Microbiology. 2000. doi:10.1016/S1369-5274(00)00103-X

63. Perfect JR, Ketabchi N, Cox GM, Ingram CW, Beiser CL. Karyotyping of Cryptococcus neoformans as an epidemiological tool. J Clin Microbiol. 1993. doi:10.1128/jcm.31.12.3305-3309.1993

Figure Legends

Figure 1. Effect of Glycolysis Inhibitors on Titan Cell Formation in *C. neoformans*:
(A) Schematic overview of glycolysis and its inhibition by glycolysis inhibitors (2-Deoxy-D-Glucose (2DG) and sodium citrate (NaCi)). (B) Wild-type strain was cultured in Titan cell medium (TCM) with and without inhibitor (2DG (0.025%)) at 37°C with 5% CO_2 for 72 hours. Cells were fixed and imaged using Zeiss Apotome microscope. Percentage of Titan cells was quantified as a ratio of cells with diameter ≥10 µm to total number of cells (≥5 µm). Cell diameter was measured using Zen 2.3 software. Threshold for cell body diameter of Titan cells is indicated by the red line. More than 200 cells were counted for each condition. Statistical analysis was done using unpaired t-test, ***(P<0.001) and **(P<0.01). Error bars represent SEM. Scale bars represents 2 µm. (C) Wild-type strain was cultured in TCM with and without inhibitor (NaCi (0.5%)) at 37°C with 5% CO_2 for 72 hours. Cells were fixed and imaged using Zeiss Apotome microscope. Percentage Titan cells was quantified as a ratio of cells with diameter ≥10 µm to total number of cells (≥5 µm). Cell diameter was measured using Zen 2.3 software. Threshold for cell body diameter of Titan cells is indicated by the red line. More than 200 cells were counted for each condition. Statistical analysis was done using unpaired t-test, ***(P<0.001) and **(P<0.01). Error bars represent SEM. Scale bars represents 2 µm. (D) Growth curve was performed to monitor overall growth of wild-type strain on TCM, +2DG and +NaCi conditions. Overnight grown culture of wild-type strain was diluted to OD_{600}=0.01 in fresh TCM medium with and without 2DG (0.025%) or NaCi (0.5%) and allowed to grow at 37°C for 24 hours. OD_{600} was recorded at 3 hour intervals. (E) For capsule visualization, wild-type strain was cultured in TCM with and without 2DG at 37°C with 5% CO_2 for 72 hours, cells were stained with India Ink and imaging was done using Zeiss Apotome microscope. Total cell diameter was measured using Zen 2.3 software. Approximately 150 cells were counted for each condition. Statistical analysis was done using unpaired t-test, ***(P<0.001). Error bars represent SEM. Scale bars represents 2 µm. (F) For capsule visualization, wild-type strain was cultured in TCM with and without NaCi at 37°C with 5% CO_2 for 72 hours, cells were stained with India Ink and imaging was done using Zeiss Apotome microscope. Total cell diameter was measured using Zen 2.3 software. Approximately 150 cells were counted for each condition. Statistical analysis was done using unpaired t-test, ***(P<0.001). Error bars represent SEM. Scale bars represents 2 µm.

Figure 2. Genetic Perturbation of Glycolysis Attenuates Titan cell formation in *C. neoformans*:
(A) Overview of glycolysis pathway showing targeted gene deletions. (B) Wild-type, *hxk1*Δ and *hxk2*Δ strains were cultured in Titan cell medium (TCM) at 37°C with 5% CO_2 for 72 hours. Cells were fixed and imaged using Zeiss Apotome microscope. Percentage of Titan cells was quantified as a ratio of cells with diameter ≥10 µm to total number of cells (≥5 µm). Cell diameter was measured using Zen 2.3 software. Threshold for cell body diameter of Titan cells is indicated by the red line. More than 200 cells were counted for each condition. Statistical analysis was done using unpaired t-test, ***(P<0.001) and **(P<0.01). Error bars represent SEM. Scale bars represents 2 µm. (C) Wild-type and *pyk1*Δ strains were cultured in TCM at 37°C with 5% CO_2 for 72 hours. Cells were fixed and imaged using Zeiss Apotome microscope. Percentage of Titan cells was quantified as a ratio of cells with diameter ≥10 µm to total number of cells (≥5 µm). Cell diameter was measured using Zen 2.3 software. Threshold for cell body diameter of Titan cells is indicated by the red line. More than 200 cells were counted for each condition. Statistical analysis was done using unpaired t-test, ***(P<0.001). Error bars represent SEM. Scale bars represents 2 µm. (D) Growth curve was performed to monitor overall growth of wild-type and knockout strains including *hxk1*Δ, *hxk2*Δ*,* and *pyk1*Δ in TCM. Overnight grown cultures of wild-type strain and knockout strains including *hxk1*Δ, *hxk2*Δ*,* and *pyk1*Δ were diluted to OD_{600}=0.01 in fresh TCM and allowed to grow at 37°C for 24 hours. OD_{600} was recorded at 3 hour intervals. (E) For capsule visualization, wild-type, *hxk1*Δ and *hxk2*Δ strains were cultured in TCM at 37°C with 5% CO_2 for 72 hours, cells were stained with India Ink and imaging was done using Zeiss Apotome microscope. Total cell diameter was measured using Zen 2.3 software. Approximately 150 cells were counted for each condition. Statistical analysis was done using unpaired t-test, ***(P<0.001) and **(P<0.01). Error bars represent SEM. Scale bars represents 2 µm. (F) For capsule visualization, wild-type and *pyk1*Δ strains were cultured in TCM at 37°C with 5% CO_2 for 72 hours, cells were stained with India Ink and imaging was done using Zeiss Apotome microscope. Total cell diameter was measured using Zen 2.3 software. Approximately 150 cells were counted for each condition. Statistical analysis was done using unpaired t-test, ***(P<0.001). Error bars represent SEM. Scale bars represents 2 µm.

855 **Figure 3. Perturbation of Glycolysis Affects cAMP-PKA Signalling in Titan Cell Inducing**
856 **Conditions:**
857 (A) Overview of cAMP-PKA pathway regulating the expression of key genes involved in capsule formation. (B)
858 Wild-type strain, *hxk1*Δ, *hxk2*Δ, and *pyk1*Δ strains were cultured in Titan cell medium (TCM) at 37°C with 5% CO_2
859 for 72 hours. Total RNA was extracted after 72 hours and comparative RT-qPCR was performed to check the
860 relative expression of genes involved in capsule formation including *cap10* and *nrg1.* Statistical analysis was done
861 using unpaired t-test, **(P<0.01), ***(P<0.001) and ns (non-significant). Error bars represent SEM. (C) Overview
862 of cAMP-PKA pathway regulating key expression of genes involved in melanin biosynthesis. (D) Wild-type strain,
863 *hxk1*Δ, *hxk2*Δ, and *pyk1*Δ strains were cultured in TCM at 37°C with 5% CO_2 for 72 hours. Total RNA was extracted
864 after 72 hours and comparative RT-qPCR was performed to check the relative expression of genes involved in
865 melanin biosynthesis including *lac1* and *lac2.* Statistical analysis was done using unpaired
866 t-test, **(P<0.01), ***(P<0.001) and ns (non-significant). Error bars represent SEM.
867
868 **Figure 4. Glycolysis Orchestrates Titan Cell Formation in a cAMP-PKA Dependent**
869 **Manner:**
870 (A) Overview of glycolysis-dependent regulation of cAMP-PKA pathway in the context of Titan cell formation. (B)
871 Wild-type and *hxk2*Δ strains were cultured in Titan Cell Medium (TCM) in the presence and absence of cAMP (10
872 mM) at 37°C with 5% CO_2 for 72 hours. Cells were fixed and imaged using Zeiss Apotome microscope. Percentage
873 of Titan cells was quantified as a ratio of cells with diameter ≥10 µm to total number of cells (≥5 µm). Cell diameter
874 was measured using Zen 2.3 software. Threshold for cell body diameter of Titan cells is indicated by the red line.
875 More than 200 cells were counted for each condition. Statistical analysis was done using unpaired t-test, *(P<0.05),
876 ***(P<0.001) and ns (non-significant). Error bars represent SEM. Scale bar represents 2 µm. (C) Wild-type and
877 *pyk1*Δ strains were cultured in TCM in the presence and absence of cAMP (10 mM) at 37°C with 5% CO_2 for 72
878 hours. Cells were fixed and imaged using Zeiss Apotome microscope. Percentage of Titan cells was quantified as
879 a ratio of cells with diameter ≥10 µm to total number of cells (≥5 µm). Cell diameter was measured using Zen 2.3
880 software. Threshold for cell body diameter of Titan cells is indicated by the red line. More than 200 cells were
881 counted for each condition. Statistical analysis was done using unpaired t-test, *(P<0.05), **(P<0.01), ***(P<0.001)
882 and ns (non-significant). Error bars represent SEM. Scale bar represents 2 µm. (D) For capsule visualization, wild-
883 type and *hxk2*Δ strains were cultured in TCM in the presence and absence of cAMP (10 mM) at 37°C with 5% CO_2
884 for 72 hours, cells were stained with India Ink and imaging was done using Zeiss Apotome microscope. Total cell
885 diameter was measured using Zen 2.3 software. Approximately 150 cells were counted for each condition.
886 Statistical analysis was done using unpaired t-test, **(P<0.01) and ***(P<0.001). Error bars represent SEM. Scale
887 bar represents 2 µm. (E) For capsule visualization, wild-type and *pyk1*Δ strains were cultured in TCM in the
888 presence and absence of cAMP (10 mM) at 37°C with 5% CO_2 for 72 hours, cells were stained with India Ink and
889 imaging was done using Zeiss Apotome microscope. Total cell diameter was measured using Zen 2.3 software.
890 Approximately 150 cells were counted for each condition. Statistical analysis was done using unpaired t-test,
891 *(P<0.05) and ***(P<0.001). Error bars represent SEM. Scale bar represents 2 µm.
892
893 **Figure 5. Melanin Biosynthesis is Critical for Titan Cell Formation in *C. neoformans:***
894 (A) Overview of the regulation of melanin biosynthesis *via* the glycolysis-dependent cAMP-PKA pathway, in the
895 context of Titan cell formation. (B) Wild-type and *lac1*Δ strains were cultured in Titan cell medium (TCM) at 37°C
896 with 5% CO_2 for 72 hours. Cells were fixed and imaged using Zeiss Apotome microscope. Percentage of Titan cells
897 was quantified as a ratio of cells with diameter ≥10 µm to total number of cells (≥5 µm). Cell diameter was measured
898 using Zen 2.3 software. Threshold for cell body diameter of Titan cells is indicated by red line. More than 200 cells
899 were counted for each condition. Statistical analysis was done using unpaired t-test, **(P<0.01) and ***(P<0.001).
900 Error bars represent SEM. Scale bar represents 2 µm. (C) Growth curve was performed to monitor overall growth
901 of wild-type strain and knockout strain *lac1*Δ in TCM. Overnight grown culture of wild-type strain and *lac1*Δ strain
902 were diluted to OD_{600}=0.01 in fresh TCM and allowed to grow at 37°C for 24 hours. OD_{600} was recorded at 3 hour
903 intervals. (D) For capsule visualization, wild-type strain and *lac1*Δ strain were cultured in TCM at 37°C with 5% CO_2
904 for 72 hours, cells were stained with India Ink and imaging was done using Zeiss Apotome microscope. Total cell
905 diameter was measured using Zen 2.3 software. Approximately 150 cells were counted for each condition.
906 Statistical analysis was done using unpaired t-test, ***(P<0.001). Scale bar represents 2 µm.
907
908
909

Figure 6. A Conserved Metabolic Network Regulates Titan Cell Formation in *Cryptococcus neoformans*:

Active glycolysis plays a critical role in the regulation of the cAMP-PKA signalling pathway which in turn affects the regulation of virulence factors of *C. neoformans* including capsule formation, melanin biosynthesis and Titan cell formation. Perturbation of glycolysis either through glycolysis inhibitors (2DG and NaCi) or pertinent knockout strains (*hxk1*Δ*, hxk2*Δ and *pyk1*Δ), leads to a downregulation of cAMP-PKA pathway. This, in turn, affects capsule formation, melanin biosynthesis and Titan cell formation which are required for the pathogenesis of *C. neoformans*.

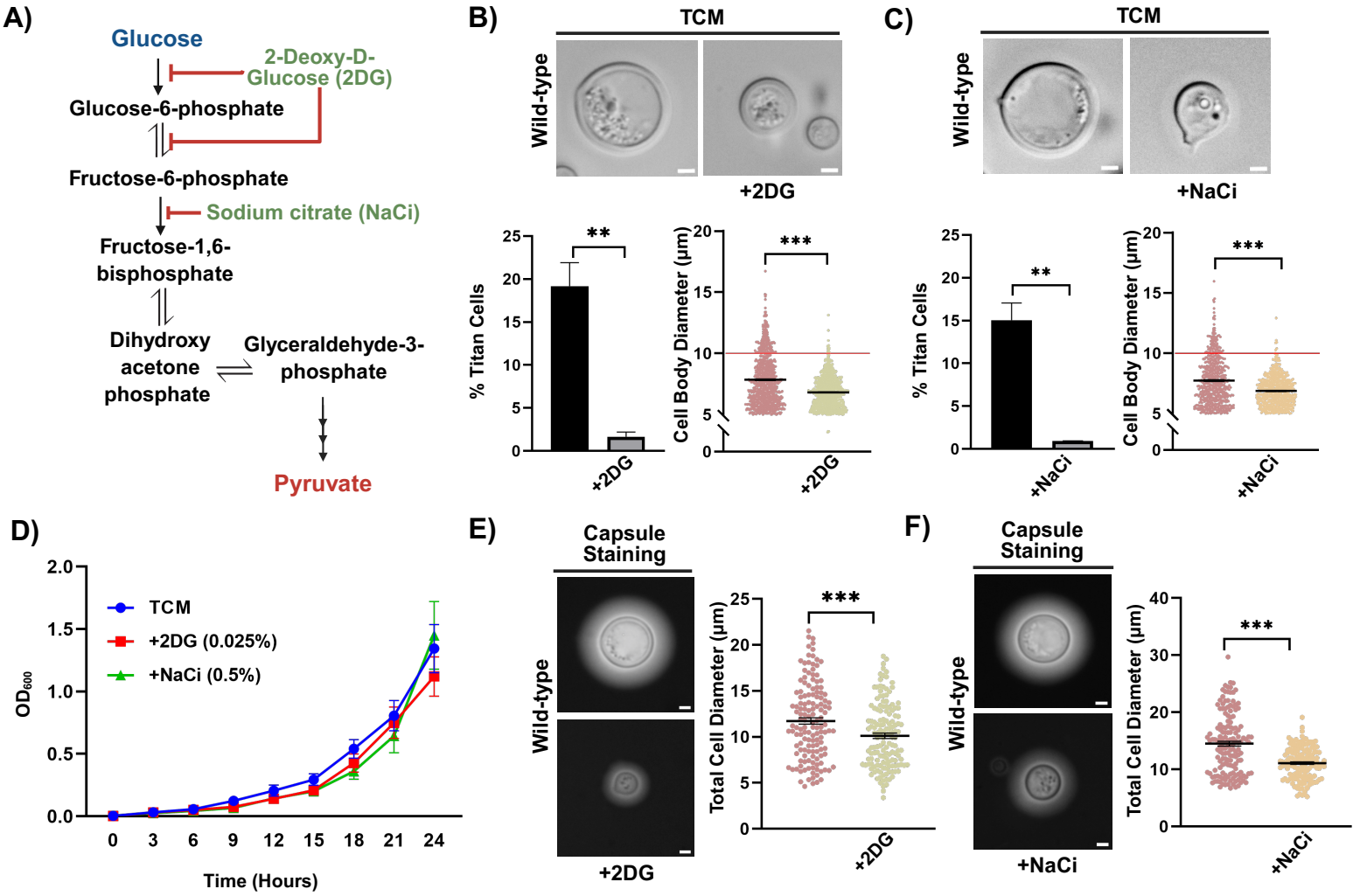
A)
Glucose
2-Deoxy-D-Glucose (2DG)
Glucose-6-phosphate
Fructose-6-phosphate
Sodium citrate (NaCi)
Fructose-1,6-bisphosphate
Dihydroxy acetone phosphate
Glyceraldehyde-3-phosphate
Pyruvate
B)
TCM
Wild-type
+2DG
% Titan Cells
Cell Body Diameter (µm)
C)
TCM
Wild-type
+NaCi
D)
TCM
+2DG (0.025%)
+NaCi (0.5%)
OD600
Time (Hours)
E)
Capsule Staining
Wild-type
+2DG
Total Cell Diameter (µm)
F)
Capsule Staining
Wild-type
+NaCi
Total Cell Diameter (µm)

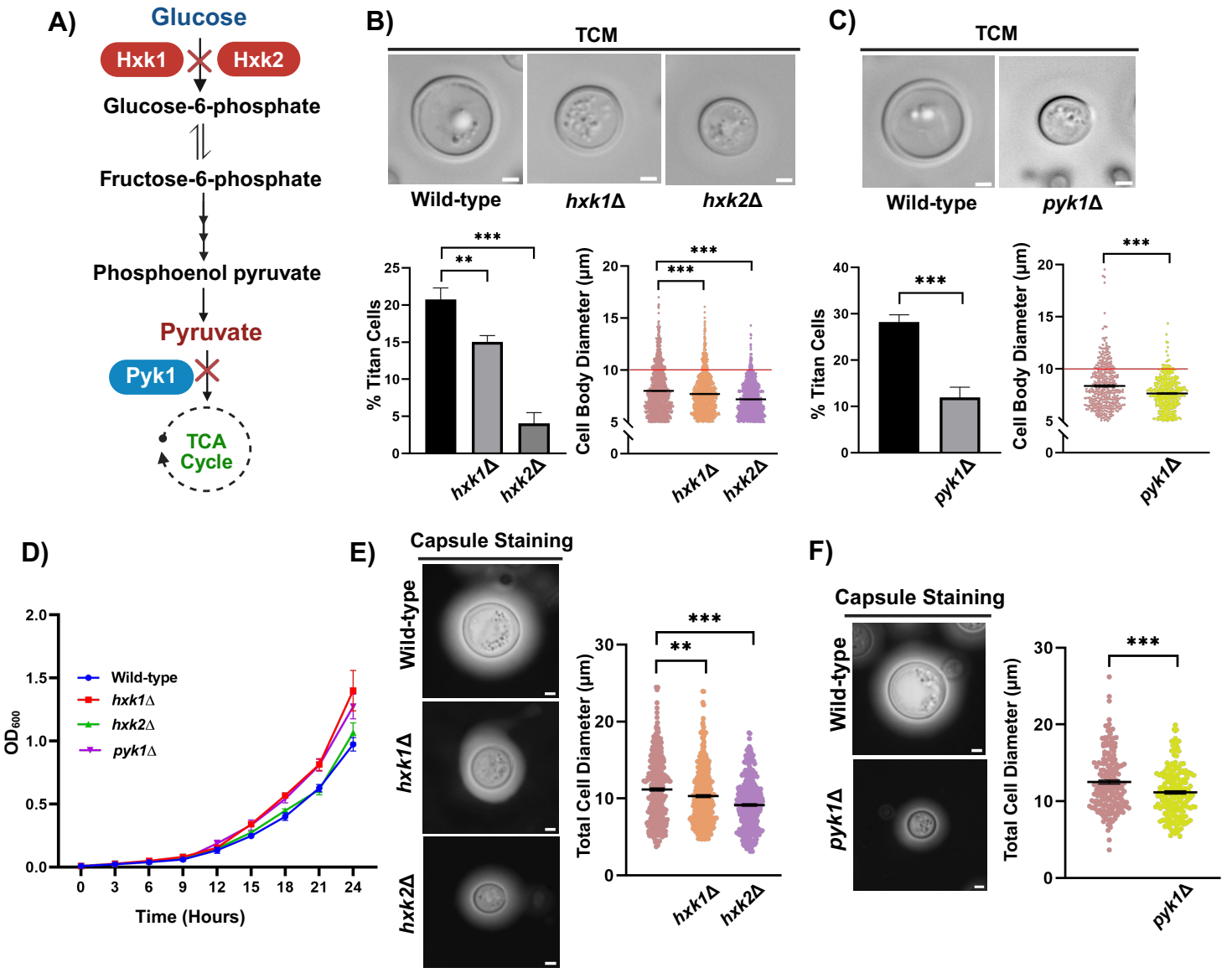
A)
Glucose
Hxk1
Hxk2
Glucose-6-phosphate
Fructose-6-phosphate
Phosphoenol pyruvate
Pyruvate
Pyk1
TCA Cycle
B)
TCM
Wild-type
hxk1Δ
hxk2Δ
% Titan Cells
Cell Body Diameter (µm)
C)
TCM
Wild-type
pyk1Δ
% Titan Cells
Cell Body Diameter (µm)
D)
OD600
Wild-type
hxk1Δ
hxk2Δ
pyk1Δ
Time (Hours)
E)
Capsule Staining
Wild-type
hxk1Δ
hxk2Δ
Total Cell Diameter (µm)
F)
Capsule Staining
Wild-type
pyk1Δ
Total Cell Diameter (µm)

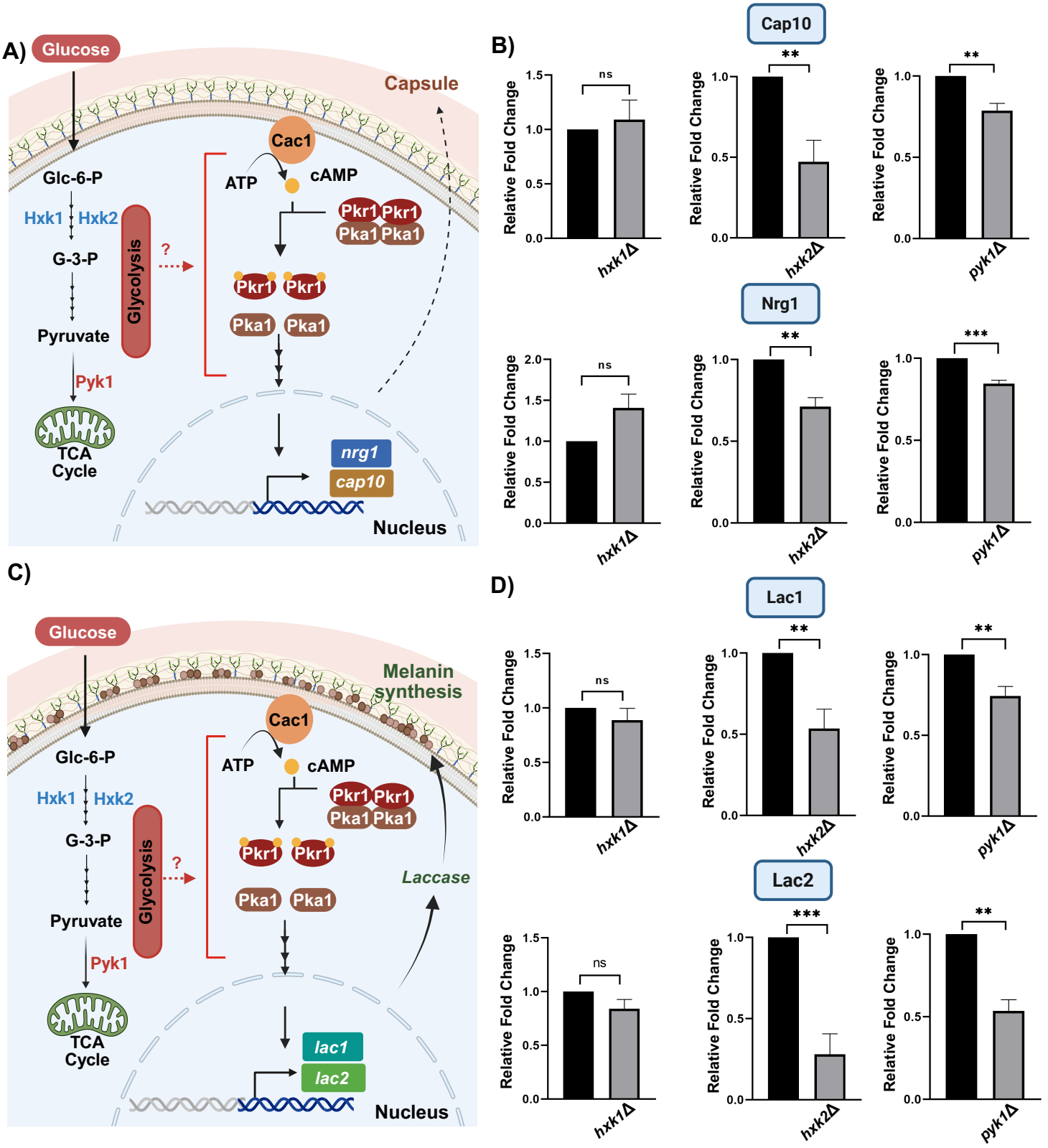
A)
Glucose
Capsule
Cac1
ATP
cAMP
Glc-6-P
Hxk1
Hxk2
Glycolysis
?
Pkr1
Pkr1
Pka1
Pka1
G-3-P
Pyruvate
Pyk1
TCA Cycle
nrg1
cap10
Nucleus
B)
Cap10
Nrg1
Relative Fold Change
ns
**
***
hxk1Δ
hxk2Δ
pyk1Δ
C)
Glucose
Melanin synthesis
Laccase
lac1
lac2
D)
Lac1
Lac2

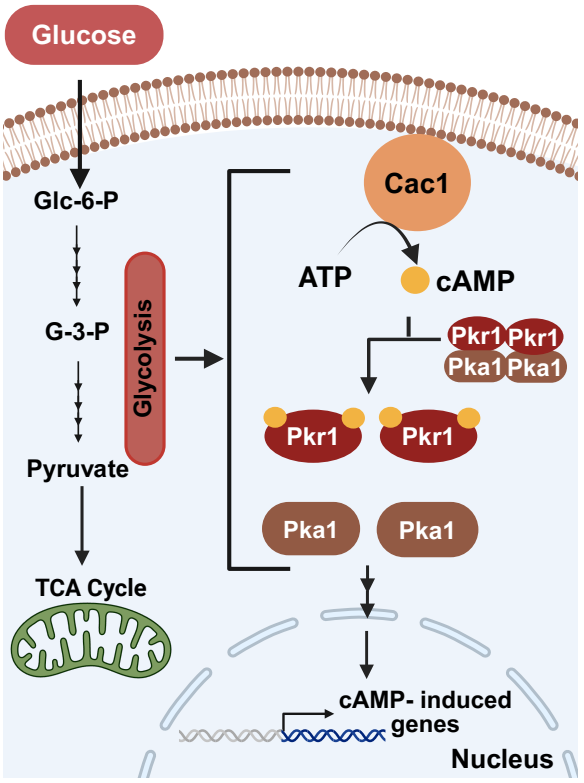
A)
Glucose
Glc-6-P
G-3-P
Glycolysis
Pyruvate
TCA Cycle
Cac1
ATP
cAMP
Pkr1
Pkr1
Pka1
Pka1
Pkr1
Pkr1
Pka1
Pka1
cAMP- induced genes
Nucleus

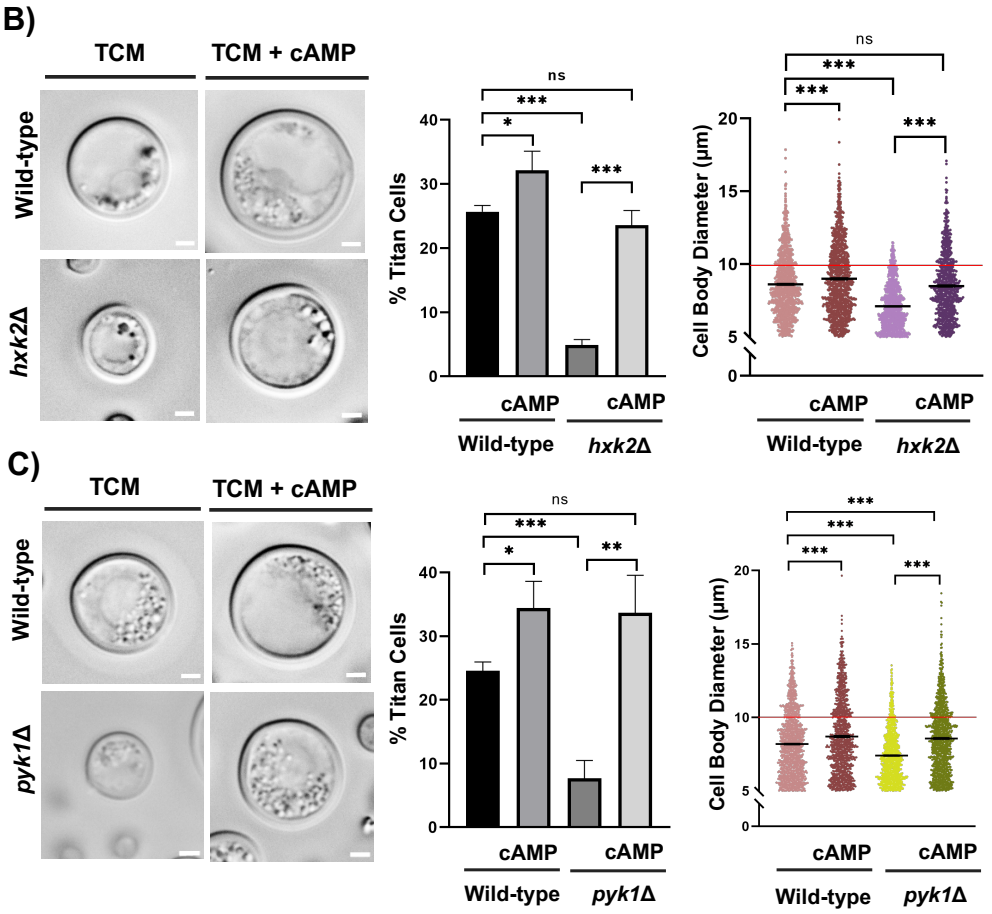
B)
TCM
TCM + cAMP
Wild-type
hxk2Δ
% Titan Cells
Cell Body Diameter (µm)
cAMP
cAMP
Wild-type
hxk2Δ
C)
TCM
TCM + cAMP
Wild-type
pyk1Δ
% Titan Cells
Cell Body Diameter (µm)
cAMP
cAMP
Wild-type
pyk1Δ

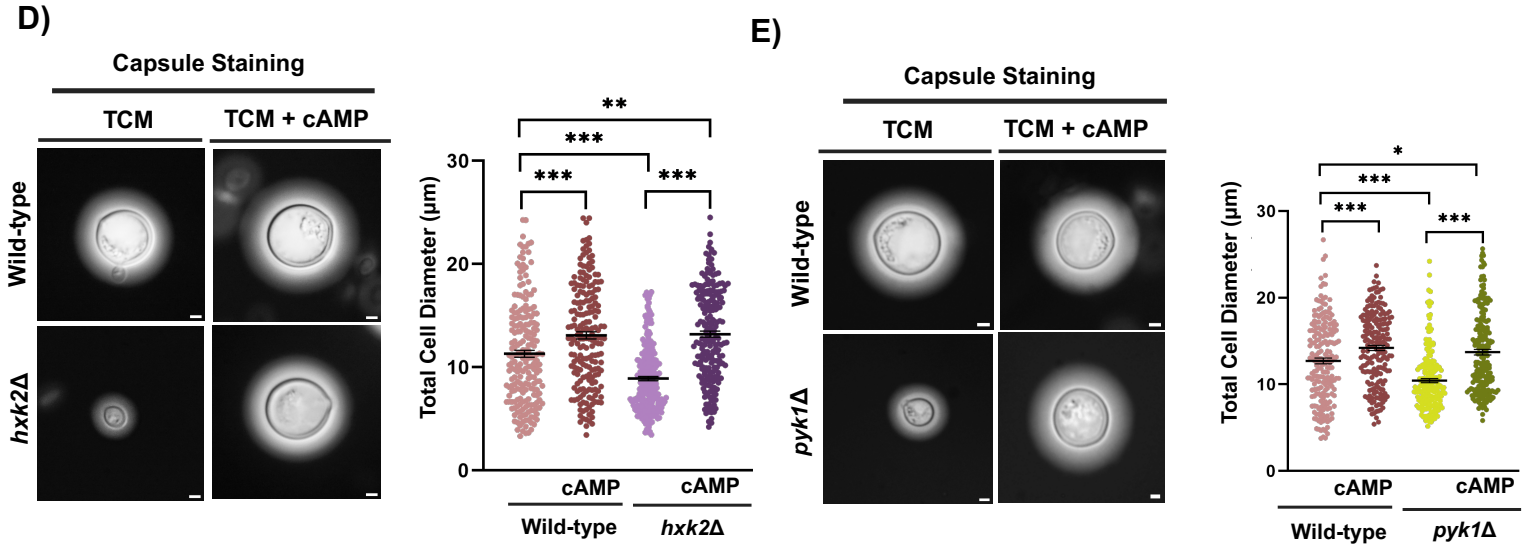
D)
Capsule Staining
TCM
TCM + cAMP
Wild-type
hxk2Δ
Total Cell Diameter (µm)
cAMP
cAMP
Wild-type
hxk2Δ
E)
Capsule Staining
TCM
TCM + cAMP
Wild-type
pyk1Δ
Total Cell Diameter (µm)
cAMP
cAMP
Wild-type
pyk1Δ

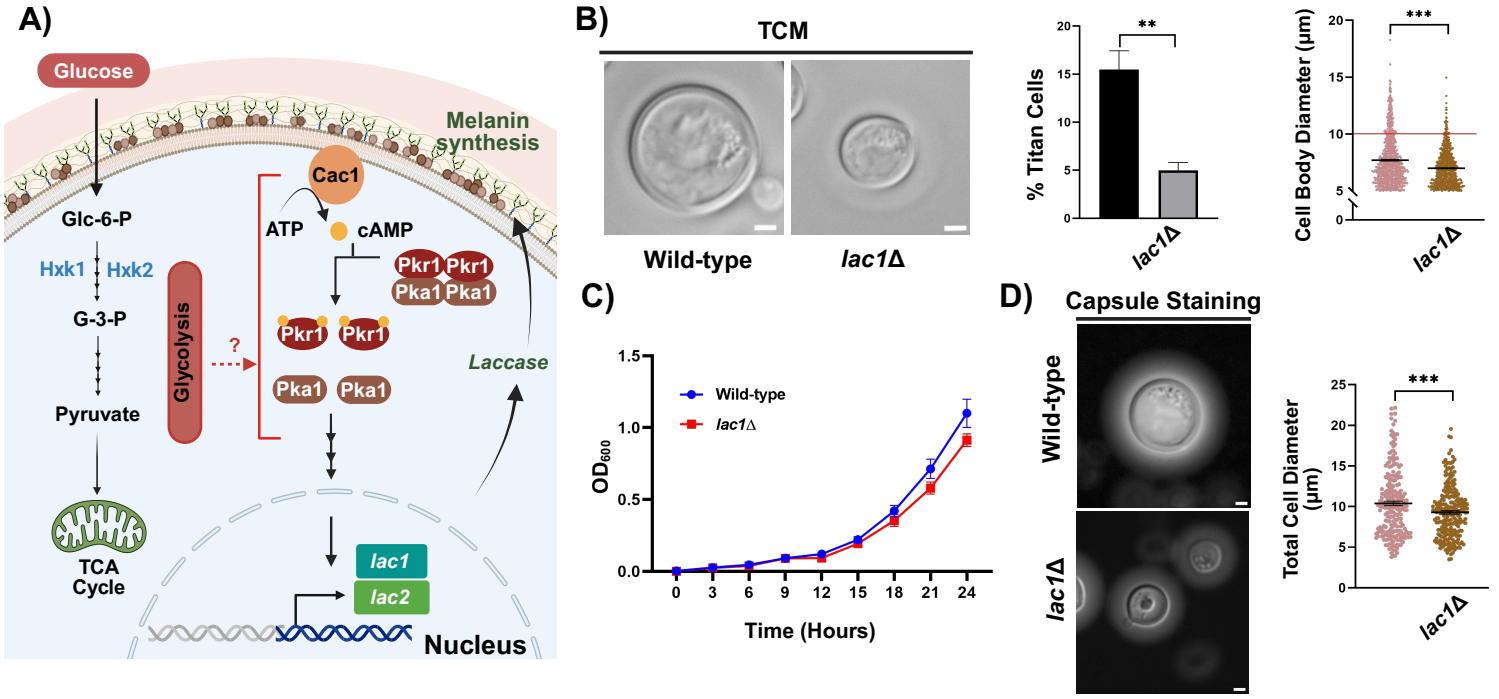
A)
Glucose
Melanin synthesis
Cac1
ATP
cAMP
Glc-6-P
Hxk1
Hxk2
G-3-P
Glycolysis
?
Pkr1
Pkr1
Pka1
Pka1
Pkr1
Pkr1
Pka1
Pka1
Laccase
Pyruvate
TCA Cycle
lac1
lac2
Nucleus
B)
TCM
Wild-type
lac1Δ
% Titan Cells
**
lac1Δ
Cell Body Diameter (µm)
***
lac1Δ
C)
Wild-type
lac1Δ
OD600
Time (Hours)
D)
Capsule Staining
Wild-type
lac1Δ
Total Cell Diameter (µm)
***
lac1Δ

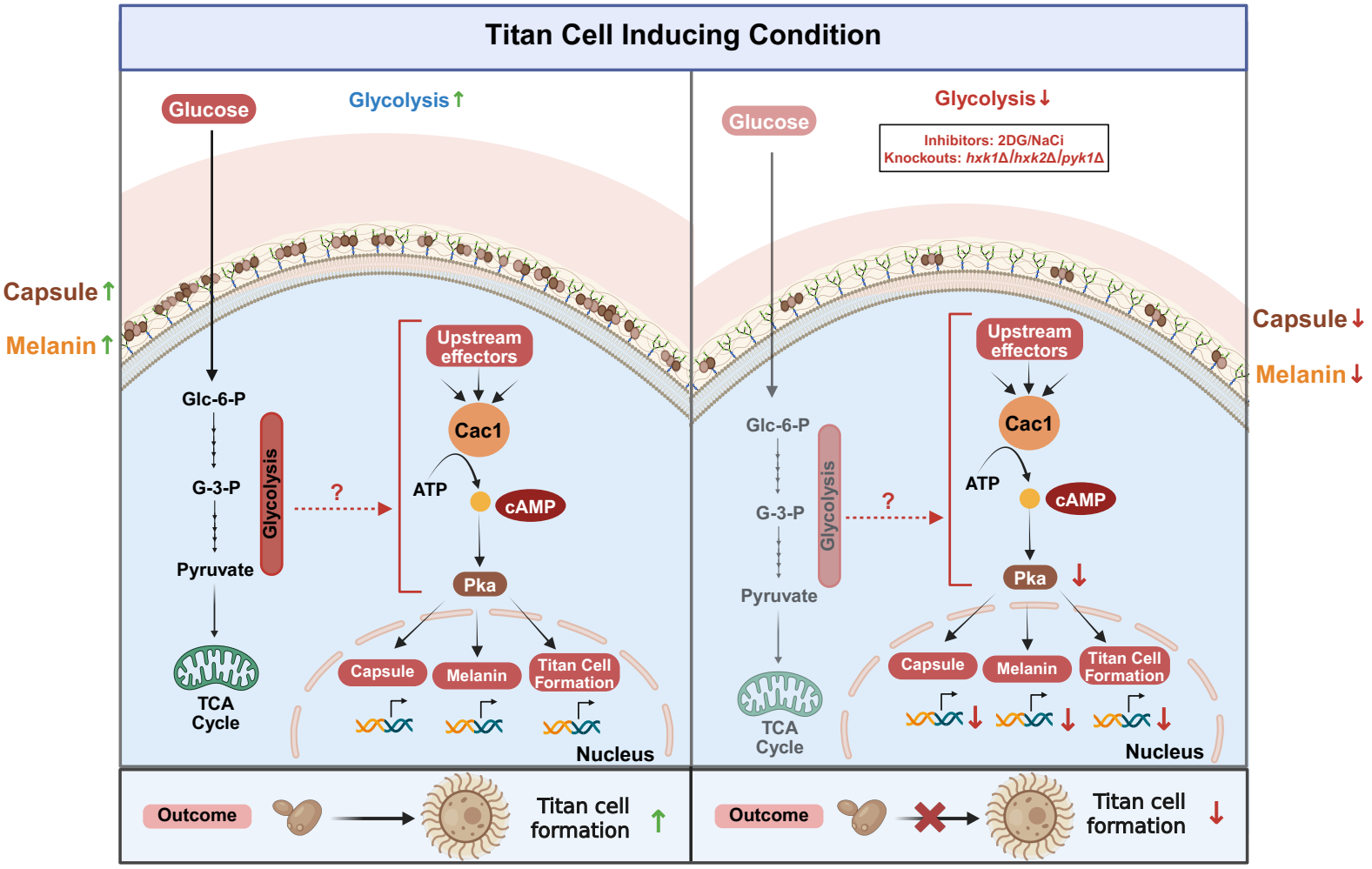
Titan Cell Inducing Condition
Glucose
Glycolysis ↑
Capsule ↑
Melanin ↑
Glc-6-P
G-3-P
Pyruvate
Glycolysis
?
Upstream effectors
Cac1
ATP
cAMP
Pka
Capsule
Melanin
Titan Cell Formation
TCA Cycle
Nucleus
Outcome
Titan cell formation ↑
Glucose
Glycolysis ↓
Inhibitors: 2DG/NaCi
Knockouts: hxk1Δ/hxk2Δ/pyk1Δ
Capsule ↓
Melanin ↓
Glc-6-P
G-3-P
Pyruvate
Glycolysis
?
Upstream effectors
Cac1
ATP
cAMP
Pka ↓
Capsule
Melanin
Titan Cell Formation
TCA Cycle
Nucleus
Outcome
Titan cell formation ↓